ARTICLE IN PRESS

Available online at www.sciencedirect.com
SCIENCE DIRECT®

Advances in Space Research xxx (2005) xxx–xxx

ADVANCES IN SPACE RESEARCH (a COSPAR publication)

www.elsevier.com/locate/asr

Coronal mass ejections associated with polar crown filaments

Guiping Zhou [a,*], Yuming Wang [b], Jingxiu Wang [a]

[a] National Astronomical Observatories, Chinese Academy of Sciences, Beijing 100012, China
[b] School of Earth and Space Sciences, University of Science and Technology of China, Hefei 230027, Anhui, China

Received 29 October 2004; received in revised form 21 March 2005; accepted 21 March 2005

Abstract

In the sample of 301 well identified earth-directed halo coronal mass ejections (CMEs) from March 1997 to December 2003, all 21 CMEs associated with polar crown filament (PCF) eruptions are analyzed. Here, the PCFs are viewed as the filaments that partially or totally lie along the boundaries of polar coronal holes, with average length over 1000″, and are intrinsically associated with extended bipole regions (EBRs). The current approach focuses on the CME properties and the flux change in the filament channels. According to the magnetic configurations where the PCFs lie, three classes of PCFs are identified. CMEs present distinguishable velocity distributions associated with each type of PCFs. About 28% of these CMEs present geoeffective. Approximately, 10^{15} Mx S^{-1} magnetic flux inflow into the filament channel and several times of 10^{20} Mx flux changed during the course of PCF eruption, which are speculated to trigger the PCF eruptions.

Keywords: Coronal mass ejections; Polar crown filaments; Extended magnetic bipoles

1. Introduction

CMEs , as big as five active regions (ARs) in average size (Hundhausen, 1999), are trigged by a sudden release of excess energy stored in the previously stable magnetic field structure (Boberg and Lundstedt, 2000). Understanding the triggering processes of CME onset should be based on large-scale magnetic field structures. The polar crown filaments (PCFs) located above the neutral lines that separate the polar magnetic regions from the large-scale magnetic cells in the medium latitudes (McIntosh, 1980). They intimately connected to large-scale magnetic structures on the photosphere, which often appear as extended bipole regions (EBRs) shown in synoptic magnetic charts. The EBRs obey Hale law in magnetic polarity distributions. An EBR often originates from several decayed ARs (Fig. 1) and involves flares, active regions and quiescent filaments, magnetic flux eruption and magnetic shearing (Feynman and Hundhausen, 1994; Feynman, 1997), which are often associated with CMEs. Most CMEs are initiated within the same type of large-scale, well organized, magnetic field regions (Hundhausen, 1988).

The PCFs may present a type of large-scale magnetic structure. The difference in such magnetic structures are speculated to affect the PCF eruptions and the associated CME properties. To enlarge the samples in this work, the PCFs are viewed as the filaments which partially or totally lied along the boundaries of polar coronal holes. Such a PCF above long neutral line over approximately 1000″ on average, appears to extend its body from the plage region to possible AR, outline large-scale structure involved in the process of CME. AR activity often is involved in such PCF activity, which probably facilitates their eruptions. Based on the work of Zhou et al. (2003), 301 earth-directed halo CMEs are identified from March 1997 to December 2003 and total of 21 CMEs associated with polar crown

* Corresponding author. Tel.: +86 10 64 888 707; fax: +86 10 648 51469.
E-mail address: zhougp@ourstar.bao.ac.cn (G. Zhou).

0273-1177/$30
doi:10.1016/j.asr.2005.03.110

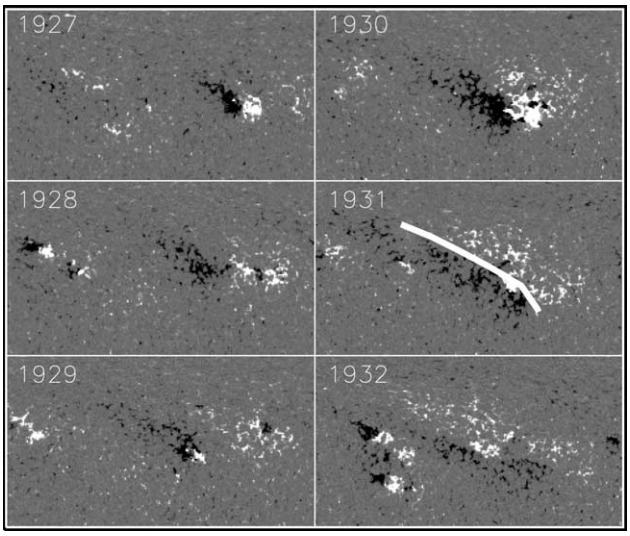

Fig. 1. An EBR evolution, the white line indicates a PCF.

filament eruptions are analyzed. A classification is tried to categorize the PCFs based on their background magnetic structures. It is also found that the CMEs present regular velocity distributions. Using the daily magnetograms after rotation and projection modifications, the magnetic flux changes in the filament channels are carefully estimated. The study is based on the SOHO LASCO, EIT and MDI time-lapse observations, as well as MDI synoptic charts and Hα images from BBSO, MEUD, Kisf and Kanz. To examine the CME interplanetary counterparts, the data from the spacecrafts WIND and ACE are also surveyed.

In the following section, PCF categorizations and the associated CME distinguishable characteristics will be introduced. The magnetic flux changes in the PCF channels during the eruptions are presented in Section 3. The discussion and conclusion is given in Section 4.

2. PCF categorizations and properties of the associated CMEs

It has been found that all the PCFs are connected with some types of EBRs which can be seen clearly in MDI synoptic magnetic charts. According to the locations of the PCF-associated magnetic inversion lines on the photosphere, the PCFs are categorized into three groups: G1, in an EBR; G2, between two EBRs; G3, totally between polar coronal hole and the following polarity flux of activity bets, for which the filament magnetic channels are almost parallelled to the solar equator. As shown in Fig. 2, using the contour of MDI data overlying the corresponding Hα images, these three groups can be easily identified. The filaments are indicated by the arrow bars. To distinguish the neutral lines from the background noisy signal, an approach smooths

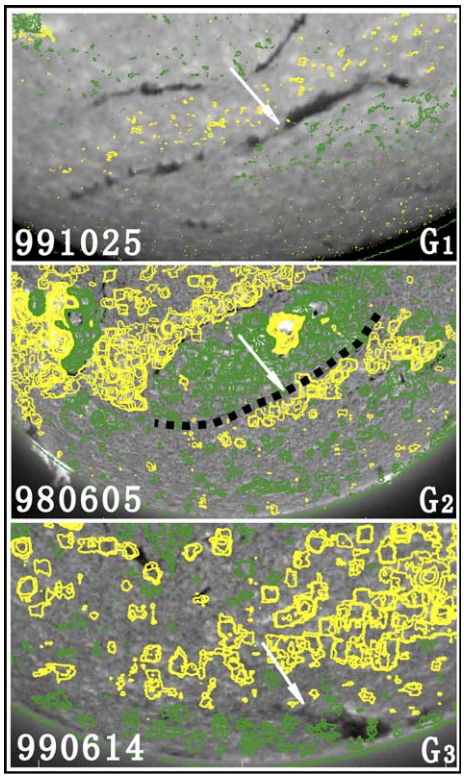

Fig. 2. Three categorizations of PCFs: G1–G3.

the MDI data with 15 pixels and make the images within a restricted range of intensities till the neutral lines of the filaments can be seen in the MDI image (see the lower two images of Fig. 2).

The associated CMEs present regular velocity distributions among these three groups (see Fig. 3). To G1, PCF above the neutral line of an EBR on the photosphere, most of the associated CMEs are slow. To G2, the PCFs erupt between two EBRs, their associated

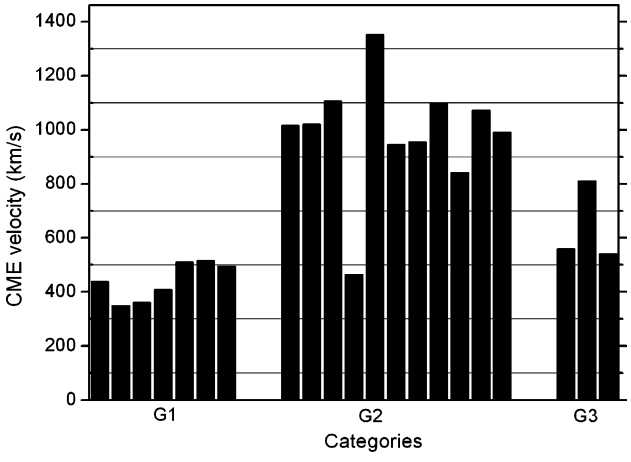

Fig. 3. The associated CME velocity distributions in G1–G3.

CMEs mostly are fast. To the last category G3, PCFs totally between polar coronal hole and the following polarity flux of activity bets, their zero lines often parallel to the solar equator. Their associated CMEs include both slow and fast ones. CMEs are the most important solar events affecting the geo-space environment and driving the disastrous space weather (Gosling, 1993). The interplanetary effects of these CMEs, i.e., ''interplanetary coronal mass ejections'' (ICMEs) or magnetic clouds (MCs), are also examined. The principle method for identifying potential ICMEs is the same as that of Cane and Richardson (2003). As a result, six CMEs may have geoeffectiveness, which occupy about 28% of all such CMEs. Among them, 4 CMEs may cause large geomagnetic storms with the K_p index $\geqslant 5^+$.

In conclusion, most of fast CMEs are related to the eruptions of PCFs between two nearby EBRs. While the PCFs erupt in one EBR, their corresponding CMEs probably are slow. To Group G3, which are very close to polar regions, their associated CMEs cannot be concluded as fast or slow. There is less than 1/3 CMEs associated PCF eruptions may have geoeffectiveness, and about 1/5 may cause large geoeffective storms, which indicate that the geoeffectiveness of such high latitude CMEs cannot be neglected.

3. Magnetic evolutions during the course of PCF eruptions

Long filaments with lower temperature suspend in the corona above the magnetic neutral lines, whose eruptions are suspected to connected with magnetic flux evolution in the magnetic channel. In this work, a filament magnetic channel points to the magnetic inversion zone, which is the position where the PCF is projected on the photosphere. The width of such channel is often thought of as 50″ in Hα observations, while 100″ averagely in EIT images (Aulanier and Schmieder, 2002). So in the MDI magnetograms, 80″ is considered as the width of the PCF channel.

Two kinds of magnetic flux change are calculated based on the MDI magnetograms. One is about the inflow flux into magnetic channel on the photosphere, above which the PCFs bestride. The other is the absolute magnetic flux change in the channel. To reduce the noise signals and projection effects, only some events near the disk center are chosen to calculate. A PCF eruption on May 8th 2000 was chosen as a case to analyze the magnetic evolution. The PCF erupted at about 14:00 UT. Using the method of local correlation tracking (November and Simon, 1988; Nindos and Zhang, 2002) based on the daily MDI magnetograms, we calculate the inflow flux into the magnetic inversion zone from 12:47 to 14:27 UT during which the filament began to erupt. As indicated in Fig. 4, the PCF channel is denoted by the two long solid lines. Its width is 80″. The length and arrow of the short bars in the magnetic channel represent the value and directions of the moving magnetic elements respectively (Fig. 4). The result shows that there are about 1.9×10^{15} Mx S^{-1} in this interval inflow into the inversion zone.

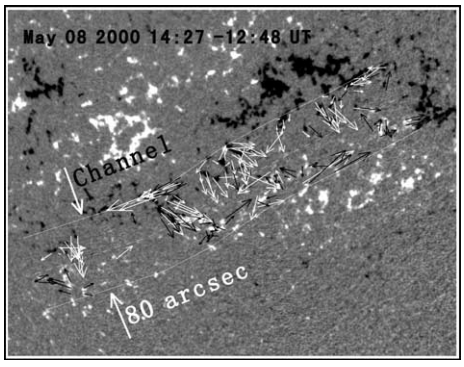

Fig. 4. The velocity sketch of magnetic elements in the inversion zone.

Magnetic flux change in the channel from 01:30 UT to 16:03 UT is estimated. During calculating, two modifications about MDI data are applied. The first is improving its precision by the referred Kitt Peak magnetic data, which has higher resolution and lower noise than MDI data. The total absolute magnetic flux of each magnetogram in a day is considered same. Then a coefficient can be obtained by using the total absolute magnetic flux of the Kitt Peak magetogram dividing by that of the MDI magnetogram. The MDI data is modified after multiplying the coefficient. The second is removing the projection effects in the light of sight by the method of Wood and Martens (2003). The modified new image has each pixel represented by the same surface area on the photosphere.

Based on such modifications of MDI data, the coalescent or fragmental flux of each magnetic element in the field of vision in the inversion zone are calculated. The results are shown in Table 1. Total magnetic flux change is 2.7×10^{20} several past 10 h before the PCFs eruption in the inversion zone. Since too much projection effects and short of high resolution magnetic field observations, it is very difficult to calculate the magnetic flux change for each event. However, based on the data modifications, it is certain for the magnitude order of the estimated magnetic flux in the inversion zone.

Table 1
Flux change in filament's channel on May 8 2000

Polarity	Coalescent flux	Fragmental flux	Change
Positive	6.49×10^{19}	5.06×10^{19}	1.2×10^{20}
Negative	-6.48×10^{19}	-8.72×10^{19}	1.5×10^{20}
Total change	2.7×10^{20}		

4. Discussion and conclusion

In the 301 halo CMEs from March 1997 to December 2003, all 21 halo CMEs are found to be associated with the eruptions of PCFs near the polar regions, which occupy about 7% of all the earth-directed halo CMEs. The PCFs are categorized into three groups (G1–G3) by their large-scale background magnetic configurations on the photosphere. Their associated CMEs present distinguishable characteristics in each category. CMEs correlated the eruptive PCFs between two EBRs probably are fast, while associated with the eruptive filaments over the neutral line of an EBR mostly are slow.

The PCF-associated CMEs seem to represent a type of CMEs. As the PCFs themselves are large-scale magnetic structures which seem to be comparable to an average CME, their eruptions appear to well signal the CME initiations. In all, as CMEs are intrinsically correlated with the large-scale magnetic structures, more emphasis should be paid on the large-scale magnetic source of CMEs.

The interplanetary effects of these high latitude CMEs are also examined. About 28% of them have interplanetary counterparts, and about 1/5 cause large geomagnetic storms with K_p index $\geqslant 5^+$. They have less geoeffectiveness than the normal earth-directed CMEs, among which 45% have geoeffectiveness (Wang et al., 2002). The main reason may be that CMEs are edge events whose propagations are offset to the earth, however, their geoeffectiveness can't be neglected. It could not be excluded that the intrinsic magnetic structure, say the orientation of their magnetic arcades, of polar crown filaments in this solar cycle may constrain the geoeffectiveness of these CMEs. We will confirm this speculation with more investigations.

No large-scale flux emergence in the PCFs projected channel was identified. Instead, we often observe flux coalescence and fragmentation. Sometimes flux patches were seen to show up by coalescence, while shrunk below the detecting limit by fragmentation. A rate of 10^{15} Mx S^{-1} flux inflow into the magnetic channels during the course of filament eruption is found. The net flux changes in the neutral channel plus the inflow flux suggest that about 10^{20} Mx flux disappeared in the PCF channel during an interval $\sim$10 h before the filament eruption. If the flux shrunk down below the detection limit is ignored, such disappearing magnetic flux is assumed to be used to provide the magnetic energy for the ascending PCFs or trigger their eruptions.

Acknowledgments

The work is supported by the National Natural Science Foundation of China (G10243003 and G100233050) and the National Key Basic Science Foundation (TG2000078404).

References

Aulanier, G., Schmieder, B. The magnetic nature of wide EUV filament channels and their role in the mass loading of CMEs. A&A 386, 1106–1122, 2002.

Boberg, Fredrik, Lundstedt, Henrik Coronal mass ejections detected in solar mean magnetic field. GeoRL. 27, 3141B, 2000.

Cane, H.V., Richardson, I.G. Interplanetary coronal mass ejections in the near-Earth solar wind during 1996C2002. J. Geophys. Res. 108, 1156, 2003.

Feynman, J.. in: Crooker, N., Joselyn, JA, Feynman, J (Eds.), Coronal Mass Ejections, vol. 99. AGU, p. 49, 1997.

Feynman, J., Hundhausen, A.J. Coronal mass ejections and major solar flares: the great active center of March 1989. J. Geophys. Res. 99, 8451, 1994.

Gosling, J.T. The solar flare myth. J. Geophys. Res. 98, 18937–18950, 1993.

Hundhausen, A.J. The origin and propagation of coronal mass ejections, in: Pizzo, V.J., Holzer, T.E., Sime, D.G. (Eds), Proceeding of the Sixth International Solar Wind Conference, NCAR/TN 306+Proc, p. 181, 1988.

Hundhausen, A. Coronal mass ejections. in: Keith, T.S., Julia, L.R. et al. (Eds.), The Many Faces of the Sun. Springer, New York, 1999, p. 143.

McIntosh, P.S. Solar and interplanetary dynamics, in: Dryer, M., Tandberg-Hanssen, E. (Eds.), Proceedings of IAU Symposium. vol. 91, p. 25, 1980.

Nindos, A., Zhang, H. Photospheric motions and coronal mass ejcetion productivity. ApJ 573, 133–136, 2002.

November, L.J., Simon, G.W. Precise proper-motion measurement of solar granulation. ApJ 333, 427, 1988.

Wood, P., Martens, P. Measurements of flux cancellation during filament formation. SoPh 218, 123–135, 2003.

Wang, Y.M., Ye, P.Z., Wang, S., Zhou, G.P., Wang, J.X. A statistical study on the geoeffectiveness of Earth-directed coronal mass ejections from March 1997 to December 2000, JGRA., 107k.SSH2W, 2002.

Zhou, G.P., Wang, J., Cao, Z.L. Correlation between halo coronal mass ejections and solar surface activity. A&A 397, 1057C1067, 2003.